

Full Length Research Paper

Long-term characterization of sea conditions in the South China Sea

Osinowo Adekunle Ayodotun^{1*}, Xiaopei Lin¹, Zhao Dongliang¹ and Wang Zhifeng²

¹College of Physical and Environmental Oceanography, Ocean University of China, Qingdao, 266100, China.

²College of Engineering, Ocean University of China, Qingdao, 266100, China.

Received 19 March, 2016; Accepted 24 March, 2016

Abstract

Wave simulation was conducted for a 30 year (1976-2005) period over some fourteen major locations in the South China Sea (SCS) using the wave model WAVEWATCH III. Comparisons of significant wave height (SWH) between simulation and Topex/Poseidon altimeter data showed good agreement. Based on the SWH data obtained over the above locations, a subsequent characterization of the sea states over the main regions of the SCS which are the northern, central and southern SCS was carried out. Results in all seasons showed that in the northern SCS, the slight sea state ($0.5 \leq h_s \leq 1.25$) has the highest frequency of occurrence. The smooth (wavelets) sea state ($0.1 \leq h_s \leq 0.5$) prevailed in the southern SCS while both the moderate ($1.25 \leq h_s \leq 2.5$) and slight sea states prevailed in the central SCS.

Key words: Significant wave height; South China Sea, Simulation, WAVEWATCH III (WW3); Sea state

INTRODUCTION

The South China Sea (SCS) is remarkably the deepest and largest sea around China with an average water depth of 1212 m and a maximum depth of 5567 m. After the Coral Sea and Arabian Sea, it is the third largest epicontinental sea in the global oceans. The SCS is a half-enclosed tropical sea within complex topography between the Asian landmass to the north and west, the Philippine Islands to the east, Borneo to the southeast, and Indonesia to the south (Chu and Cheng, 2004). The water volume is 3.5–3.85 million cubic square meters, which is about 13 times that of the total volume of the East China Sea, the Yellow Sea, and the Bohai Sea. The SCS is under the influence of monsoon winds and synoptic systems such as fronts and tropical cyclones (Chu and Cheng, 2004; Veneziano and Fan, 2000). Surface waves are formed when winds blow across the water surface transferring their energy to the water. As

surface winds over the ocean might be changing both in strength and patterns due to climate change, ocean waves could be affected by anthropogenic forcing of the climate system (Wang *et al.*, 2004). Ocean wind-waves are relevant for numerous engineering and scientific questions, both in coastal zones and in the deep ocean.

Analysis of the sea states over the SCS is necessary in an attempt to provide references for the wave energy resources development, navigation, marine engineering, disaster prevention and reduction.

In oceanography, a sea state is the general condition of the free surface on a large body of water with respect to wind waves and swell at a certain location and moment. A sea state is characterized by statistics, including the wave height, period, and power spectrum. The sea state varies with time, as the wind conditions or swell conditions change. The sea state can either be assessed by an experienced observer, like a trained mariner, or through instruments like weather buoys, wave radar or remote sensing satellites.

The large number of variables involved in creating the

sea state cannot be quickly and easily summarized, so simpler scales are used to give an approximate but concise description of conditions for reporting in a ship's log or similar record.

In engineering applications, sea states are often characterized by the following two parameters: The significant wave height $H_{1/3}$ — the mean height of the one third highest waves. The mean wave period, T_1 . The sea state is in addition to these two parameters (or variation of the two) also described by spectrum $S(\omega, \Theta)$ which is the product of a wave height spectrum $S(\omega)$ and a wave direction spectrum $f(\Theta)$. The dimension of the wave spectrum is $\{S(\omega)\} = \{Length^2 Time\}$, and many interesting properties about the sea state can be found from the spectrum.

Wave spectrum describes a sea state in terms of the linear random wave model by specifying a wave spectrum, which determines the energy in different frequency. As to the offshore constructions in the deep area of SCS, spectrum analysis methods are necessary in the research of dynamic response and vibration control. (Rodriguez and C. Guedes, 2000) used the Ochi-Hubble spectrum with 9 different parameterizations representing 3 types of sea state categories: swell, wind-sea dominated and mixed wind-sea and swell system with comparable energy. Each category is represented by 3 different models between the swell and the wind-sea spectral components. Combined wind-sea and swell sea states are discussed in these literatures (Strekalov and Massel, 1971; Torsethaugen, 1996).

Knowledge of wave characteristics is essential for the planning, design and construction of new ports coastal protection constructions, harbors and navigational channels [Schneggenburger *et al.*, 2000; Sundar and Ananth, 1988] and it also contributes to fisheries activities, navigation, marine habitat management and coastal development and planning.

(Saleh *et al.*, 2010) used 8 years monthly wave height and wave period data of some offshore locations in Sabah waters collected from the meteorological department, Sabah branch to identify and compare the wave characteristics in the region at five different key locations so as to determine the effects of the Northeast Monsoon (NEM) and the Southwest Monsoon (SWM) along the east and west coasts of the region. The data was analyzed at different areas through the Probability Density Function (PDF) to estimate the most likely wave height and wave period in the study area. They concluded that the range of wave heights in coastal waters surrounding Sabah was found to be 0.5-2 m. Wave height is usually higher than 1 m in the west coast during NEM while the east coast has a wave height of ~0.5 m for both monsoons.

The objectives of this paper are to establish the seasonal sea conditions and significant wave height (hs) curves with respect to the regions of some chosen locations in the SCS based on the data sets obtained from numerical

simulations from 1976 to 2005.

The paper is organized as follows. Section 2 provides information on the wave model setup and a thorough validation with altimeter data using some statistical tests with their results.

Section 3 presents the methodologies used in sea states characterization and detailed discussion on results obtained. Finally, conclusions of this study are given in section 4.

MODELS, DATA SETS AND METHODOLOGY

The wave model and input data

The model used for wave simulation is version 3.14 of the third-generation spectral wave model WAVEWATCH III™ (denoted as WW3), (Tolman, 2009). WW3 was developed at the Ocean Modeling Branch of the Environmental Modeling Center of the National Centers for Environmental Prediction (NCEP) for the regional sea wave prediction. It was built on the base of Wavewatch-I and Wavewatch-II as developed at the Delft University of Technology, and NASA Goddard Space Flight Center, respectively [16]. By using the NGDC (National Geophysical Data Center) ETOPO 1 data, with a resolution of $0.5^\circ \times 0.5^\circ$, the SCS water depth field was processed by the Gridgen 3.0 packet. Source terms for energy spectra in the model are set to default. The model integrates the spectrum to a cut-off frequency, and above this frequency a parametric tail is applied. The boundary condition is cyclical. The other option settings are 36 directions, and 24 discrete wave-numbers (0.0412 ~ 0.4060Hz, 2.4 ~ 24.7s). The model spatial grid covers the whole of SCS and part of ECS from longitudes 95°E to 135°E and latitudes 5°S to 30°N with a 0.25° resolution. The model in an operational/forecasting mode, was forced with 6hour re-analysis wind fields extracted over longitudes 95°E to 135°E and latitudes 5°S to 30°N from the WRF model from 1976 to 2005 on a 0.2° (longitude) by 0.2° (latitude) Gaussian grid. Wind fields were interpolated on a regular 0.25° grid to force the model. The model output is a two-dimensional (2D) wave energy spectra obtained at each grid point with time period spanning from 1 January, 1976 to 31 December 2005 and with a 6-hour output data. The model provides output of wave parameters including wave spectra, significant wave heights ($4\sqrt{E}$), mean wavelength ($2\pi k^{-1}$), mean wave period ($2\pi k^{-1} 2\pi$), mean wave direction, peak frequency, and peak direction. The simulation provided a 6hour time series of SWH and other wave parameters over a box extending from 3°N to 23°N and 105°E to 121°E which contains main part of SCS and surrounding waters. The available satellite data used in this study served as independent observations against which the modeled values were evaluated so no assimilation procedure was employed.

Satellite data and model verification

The observation data used in this study were obtained from Topex/Poseidon (NASA/CNES) which is an official remote sensing data center that has data containing a near-real time gridded observations for significant wave height. The Topex/Poseidon satellite, jointly launched by NASA and the French Space Agency, the Center National d'Etudes Spatiales (CNES) in August 1992, carried a state-of-the-art radar altimetry system (Fu *et al.*, 1994). In addition to precise measurements of the distance

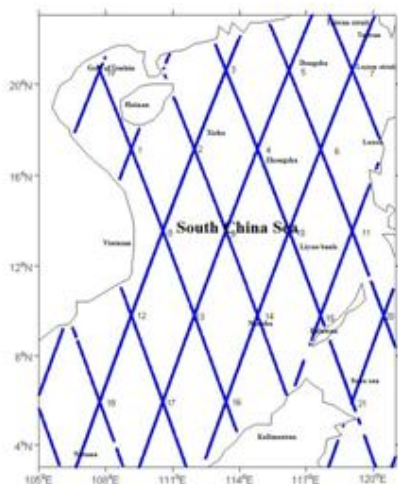


Figure 1. Topex/Poseidon crossover points and Geography of the SCS

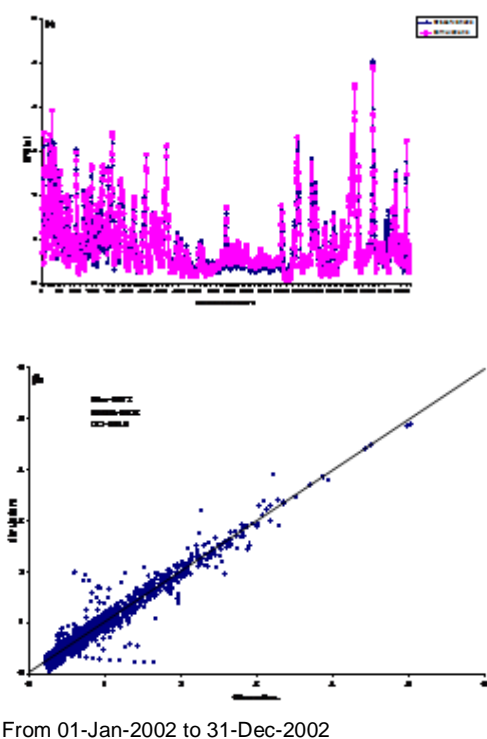


Figure 2. (a) Time series of the wave model data against Topex/Poseidon data for the SWH, on the x-axis is the number of data points. (b) Scatter plot of the wave model data against Topex/Poseidon data for the SWH.

between the satellite and the surface, SWH was derived from the shape of the leading edge of the returning radar pulse. The accuracy of SWH measurement by Topex/Poseidon was within the accuracy of the Geosat measurements [18], i.e., 10% or 0.5 m, whichever is greater

(Dobson et al., 1987). Topex/Poseidon was maneuvered into a 9.9156-day repeat period during which two Topex/Poseidon SWH data are available at each crossover point.

The TOPEX/Poseidon data was used to verify the accuracy of the WW3 simulations. The TOPEX/Poseidon satellite crossover points in the SCS in 2002 are shown in Figure.1.

The model SWH data were interpolated into all the crossover points where the hindcast and altimeter data were computed. Comparisons were conducted between the model hindcast results and the Topex/Poseidon altimeter observations. Synchronous comparisons of SWH are shown in Figures.2a and b. The time series cover different periods in, 2002 for all the crossover points as Topex/Poseidon passed over the SCS.

The skill of the model was evaluated through a conventional statistical analysis that consists on calculating the following:

$$cc = \frac{\sum_{i=1}^n (x_i - \bar{x})(y_i - \bar{y})}{\sqrt{\sum_{i=1}^n (x_i - \bar{x})^2 \sum_{i=1}^n (y_i - \bar{y})^2}} \text{-----(1)}$$

$$Bias = \bar{y} - \bar{x} \text{-----(2)}$$

$$RMSE = \sqrt{\frac{1}{N} \sum_{i=1}^n (y_i - x_i)^2} \text{-----(3)}$$

where, x_i represents the observed data, y_i represents the simulated data, \bar{x} and \bar{y} are mean values of observed and simulated data, N is the total number of observations.

The correlation coefficient (cc) between the simulated and observed data is 0.914 which indicates a close relationship between simulated and observed data. From Bias which is 0.012, we find that the model slightly overestimates the observed SWH. The RMSE between the simulated and observed data is 0.432 indicating a low error of simulated data

In general, the simulation results are consistent with the observations, which indicate that in general the WW3 can well reproduce the SWH and as well be a dependable model to simulate surface waves in the SCS.

Sea conditions in the SCS.

A thirty year SWH data obtained from simulations over fourteen selected locations listed in table 1 in the major regions of the SCS was utilized to assess the sea state of the SCS.

The information on the sea state (h_s) for the different regions of the SCS is presented as cumulative frequency $f(h_s)$ in percentage as:

$$f(h_s) = 100(n/N) \text{-----(4)}$$

Table 1. Yearly average hs for the Northern, Central and Southern SCS.

Northern SCS	hs (m)	Central SCS	hs (m)	Southern SCS	hs (m)
Dongsha	1.626	Zhongsha	1.753	Sulu sea	0.748
Gulf of Tonkin	0.583	Xisha	1.668	Palawan	1.078
Luzon strait	1.506	Liyue Bank	1.480	Nansha	1.516
Taiwan	0.809			Natuna	0.296
Average	1.131	Average	1.633	Average	0.909

Table 2. World Meteorological Organization sea state code

WMO Sea State Code	Wave height	Characteristics
0	0 metres (0 ft)	Calm (glassy)
1	0 to 0.1 metres (0.00 to 0.33 ft)	Calm (rippled)
2	0.1 to 0.5 metres (3.9 in to 1 ft 7.7 in)	Smooth (wavelets)
3	0.5 to 1.25 metres (1 ft 8 in to 4 ft 1 in)	Slight
4	1.25 to 2.5 metres (4 ft 1 in to 8 ft 2 in)	Moderate
5	2.5 to 4 metres (8 ft 2 in to 13 ft 1 in)	Rough
6	4 to 6 metres (13 to 20 ft)	Very rough
7	6 to 9 metres (20 to 30 ft)	High
8	9 to 14 metres (30 to 46 ft)	Very high
9	Over 14 metres (46 ft)	Phenomenal

Table 3. Average percentage cumulative frequency of the hs for different sea states and for the different locations.

Location	hs=0	hs≤0.1	0.1≤hs≤0.5	0.5≤hs≤1.25	1.25≤hs≤2.5	2.5≤hs≤4	4≤hs≤6	6≤hs≤9	9≤hs≤14	hs≥14
Dongsha	0	1.191	14.147	31.594	33.547	14.855	3.876	0.650	0.132	0.007
Gulf of Tonkin	0	8.000	44.786	39.483	6.846	0.563	0.205	0.101	0.015	0
Luzon strait	0	1.431	16.602	34.370	30.859	12.529	3.533	0.546	0.124	0.007
Taiwan	0	7.062	29.847	44.396	16.118	1.987	0.498	0.082	0.007	0
Zhongsha	0	0.848	12.292	33.942	29.152	15.877	6.669	1.111	0.108	0
Xisha	0	0.849	12.629	36.561	28.521	14.789	5.625	0.926	0.099	0
Liyue bank	0	2.699	15.593	33.456	31.631	13.434	2.781	0.350	0.054	0
Sulu sea	0	14.652	37.153	37.194	10.305	0.690	0.004	0	0	0
Palawan	0	4.771	20.416	40.719	28.701	4.935	0.422	0.033	0.002	0
Nansha	0	2.509	17.636	29.506	32.002	14.813	3.253	0.274	0.005	0
Natuna	0	39.674	44.944	10.667	3.783	0.834	0.0975	0	0	0

where n is the number of times hs falls within each of the defined sea states and N is the total number of hs values.

For each location and for each month in the respective years, the percentage cumulative frequency of hs has been computed for the different categories of sea states using the World Meteorological Organisation sea state code for hs in table 2. As a basis for the assessment of sea conditions, the average percentage cumulative frequency of hs for the different sea states have been computed for the locations under study. This is clearly illustrated in table 1 and figures 3(a)-(i).

Finally, the overall monthly average hs values have been computed and tabulated as shown in table 3. The monthly variation of hs for the different locations is shown Table.1 contains the yearly average hs for the northern,

central and southern regions of the SCS. It is shown from the table that the overall average hs value for the three regions are 1.131m, 1.633m and 0.909m respectively. This implies that on average, hs is higher in the central SCS that the other two regions.

Presented in figures 3(a)-(i) are the graphical interpretations of the averaged percentage cumulative frequency of hs for the different sea states in all the locations as shown in table 1. The zeros under hs=0 in table 3 is an indication that hardly there is any calm (glassy) sea condition in any of the locations. A close observation of figure 3a reveals that Natuna has the highest frequency(39.7%) in the calm (rippled) sea state category that is to say Natuna waters is more calm that that of the rest locations. Higher frequencies 44.79% and

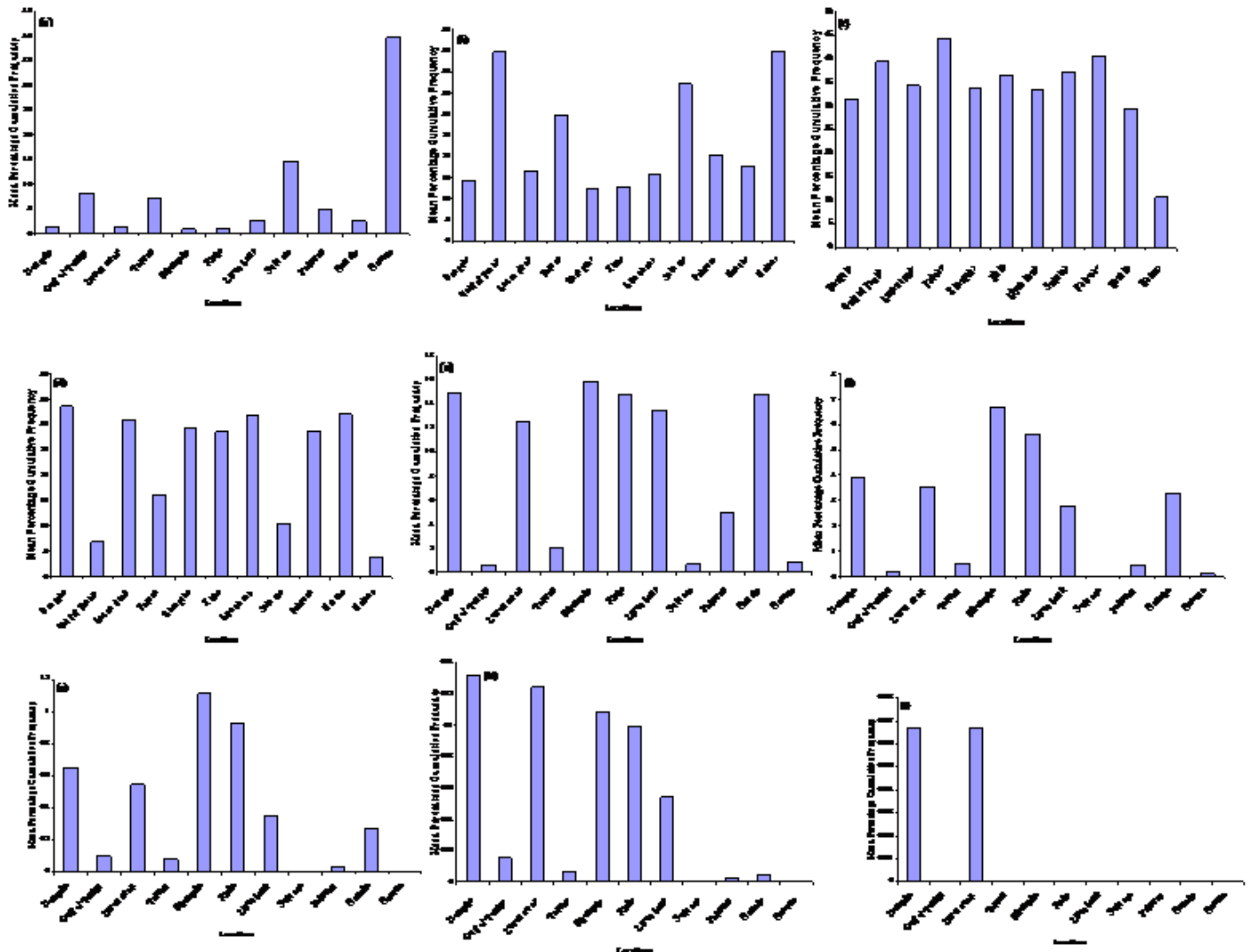


Figure 3. Plot of mean percentage cumulative frequency of months with (a) calm (rippled) 0-0.1m (b) Smooth (wavelets) 0.1 to 0.5 m (c) Slight 0.5 to 1.25 m (d) Moderate 1.25 to 2.5 m (e) Rough 2.5 to 4 m (f) Very rough 4 to 6 m (g) High 6 to 9 m (h) Very high 9 to 14 m (i) Phenomenal $\geq 14m$ sea states for the different locations.

44.94% in the smooth (wavelets) sea state category respectively exist for Gulf of Tonkin and Natuna as seen in figure 3b, this is followed by the Sulu sea(37.15%) and waters close to Taiwan(29.85%). Figure 3c shows that relatively slight sea state prevails more in Gulf of Tonkin(39.5%), Taiwan(44.4%) and Palawan(40.72%) than the other locations. It is however of least extent (10.7%) in Natuna. Moderate sea conditions as shown in figure 3d has the higher frequencies in Dongsha(33.55%), Luzon strait(30.86%), Liyue bank(31.63%) and Nansha(32%). The frequencies are least in Gulf of Tonkin(6.85%) and Natuna(3.78%). In figure 3e, the sea is rougher in Zhongsha, Dongsha, Nansha and Xisha with respective frequencies of 15.88%, 14.86%, 14.81% and 14.79% as compared with the other locations. Figures 3f and 3g show that the sea is in a very rough

and high state in Zhongsha(6.67%, 1.11%) and Xisha(5.63% , 0.93%) than any other location. Lastly, traces of very high and phenomenal sea states are noticed in Dongsha and Luzon strait as seen in figures 3h and 3i.

The overall monthly mean hs values for the different locations are contained in table 4 while the monthly variation of hs for all the locations is shown in figure 4. From this figure, it is clear that for all locations, the hs has its minimum values around May ($0.07 \leq hs \leq 0.83$) and maximum values around November, December and January in Dongsha, Gulf of Tonkin and Luzon strait ($0.65 \leq hs \leq 2.49$) which are in the northern SCS. Maximum values of hs around November, December and January are also common in Zhongsha, Xisha and Liyue bank ($1.60 \leq hs \leq 3.22$) in the central SCS. Maximum hs values

Table 4. Overall monthly average hs(m) for the different locations.

Location	Jan	Feb	Mar	Apr	May	Jun	Jul	Aug	Sep	Oct	Nov	Dec	Average(m)
Dongsha	1.993	1.743	1.289	0.926	0.827	1.278	1.469	1.584	1.416	2.032	2.492	2.465	1.626
Gulf of Tonkin	0.694	0.656	0.613	0.499	0.383	0.435	0.47	0.431	0.441	0.727	0.833	0.819	0.583
Luzon strait	1.861	1.668	1.191	0.86	0.765	1.206	1.415	1.487	1.352	1.773	2.25	2.245	1.506
Taiwan	0.797	0.726	0.542	0.406	0.467	0.945	1.089	1.193	0.885	0.831	0.929	0.896	0.809
Zhongsha	2.398	1.91	1.399	0.951	0.797	1.272	1.369	1.51	1.161	2.045	3.005	3.221	1.753
Xisha	2.287	1.837	1.365	0.932	0.754	1.153	1.239	1.344	1.071	2.003	2.931	3.098	1.668
Liyue bank	2.026	1.61	1.208	0.792	0.732	1.215	1.439	1.771	1.177	1.353	1.984	2.456	1.48
Sulu sea	1.061	0.923	0.74	0.435	0.333	0.409	0.477	0.613	0.41	0.38	2.289	0.899	0.747
Palawan	1.541	1.259	0.982	0.619	0.52	0.824	1.014	1.312	0.937	0.93	1.303	1.696	1.078
Nansha	2.596	2.041	1.492	0.874	0.627	0.976	1.159	1.462	1.028	1.161	1.997	2.784	1.516
Natuna	0.81	0.549	0.268	0.084	0.069	0.117	0.161	0.2	0.129	0.131	0.304	0.729	0.296
Average(m)	1.642	1.357	1.008	0.671	0.57	0.894	1.027	1.173	0.91	1.215	1.847	1.937	

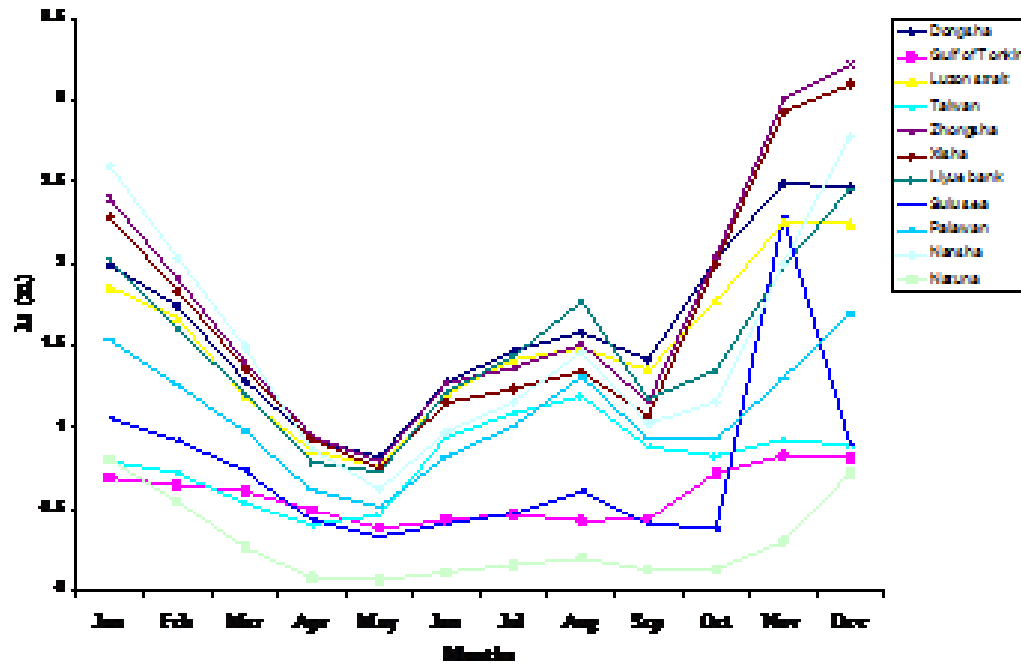


Figure 4. Monthly variation of hs for the different locations.

Table 5. Average monthly/seasonal hs values for the (a) Northern SCS, (b) Central SCS and (c) Southern SCS (*f* is computed using Equation 4).

Season	hs=0	hs≤0.1	0.1≤hs≤0.5	0.5≤hs≤1.25	1.25≤hs≤2.5	2.5≤hs≤4	4≤hs≤6	6≤hs≤9	9≤hs≤14	hs≥14	Average hs (m)
(a)											
winter	0	1.085	17.154	38.876	28.414	11.564	2.799	0.103	0.004	0	1.523
spring	0	6.562	39.057	39.545	11.961	2.45	0.366	0.035	0.022	0	0.927
summer	0	5.347	28.77	36.361	21.229	5.560	1.954	0.621	0.147	0.011	0.896
autumn	0	4.692	20.4017	35.062	25.767	10.36	2.991	0.62	0.104	0.002	1.179
(b)											
winter	0	0.06	2.613	21.062	37.427	27.772	9.846	1.202	0.018	0	2.601
spring	0	1.833	23.274	50.508	19.199	4.125	0.905	0.139	0.015	0	1.334
summer	0	2.566	16.658	36.703	31.506	9.855	2.251	0.387	0.075	0	1.108
autumn	0	1.403	11.474	30.339	30.942	17.049	7.097	1.456	0.24	0	1.493
(c)											
winter	0	2.02	19.047	31.637	33.011	11.475	2.603	0.2	0.007	0	1.501
spring	0	23.04	32.521	32.663	10.011	1.593	0.145	0.026	0	0	0.856
summer	0	19.75	34.875	25.797	14.705	4.360	0.478	0.031	0	0	0.557
autumn	0	16.8	33.705	27.991	17.065	3.843	0.550	0.05	0	0	0.725

($0.3 \leq h_s \leq 2.78$) are common in the Sulu sea, Palawan, Nansha and Natuna in November, December and January which are locations in the southern SCS. Maximum values of h_s are found during July ($h_s=1.09$) and August ($h_s=1.19$) in Taiwan. This may be due to a slight difference in sea condition in the location in comparison with the other locations in the northern SCS.

Using the annual mean values of the h_s for each location, table 4 further confirms that the sea is rougher ($1.63 \leq h_s \leq 1.75$) in Zhongsha, Xisha and Dongsha and appears to be calm ($0.29 \leq h_s \leq 0.75$) around Natuna, Gulf of Tonkin and Sulu sea. Also the relevance of h_s in the seasonal division of the SCS sea state climate is seen in the overall monthly averages of h_s for all locations at the bottom of table 4. Higher values of h_s ($1.64 \leq h_s \leq 1.94$) exist in the months of November to January during the winter monsoon and lower

values ($0.57 \leq h_s \leq 0.89$) exist in the months of April to June during the summer monsoon.

The average monthly/seasonal percentage cumulative frequency (Equation 4) of the daily h_s for the northern, central and southern SCS is shown in table 5. Statistical seasonal h_s curves for the different sea states have also been established for each of the above mentioned regions, this is seen in figures 5(a)-(c).

Figure 5a shows that in the northern SCS, the slight sea state ($0.5 \leq h_s \leq 1.25$) has the highest frequency in all seasons. The frequency is however the highest during the spring (39.6%). A little trace of a phenomenal sea state ($h_s \geq 14$) is observed in the summer and autumn.

In the central SCS (Figure 5b), the moderate sea state ($1.25 \leq h_s \leq 2.5$) occurred most of the time during the winter and autumn with respective frequencies of 37.43% and 30.94%. The slight

sea state showed the highest frequencies of 50.51% and 36.7% respectively in the spring and summer.

Lastly, the smooth (wavelets) sea state category ($0.1 \leq h_s \leq 0.5$) is particular to the southern SCS (Figure 5c) during the summer and autumn with respective frequencies of 34.88% and 33.71%. The moderate sea state occurred most of the time (33%) in the winter whereas the slight and smooth (wavelets) sea states both have the highest frequencies of 32.6% and 32.52% respectively during the spring. This on the average indicates the prevalence of the smooth (wavelets) sea state in the southern SCS.

Figures 5a-5c further confirm that the sea state curves are nearly identical in the southern SCS during winter and spring and in summer and autumn. Identical curves are also observed for the central SCS during winter and spring and in summer

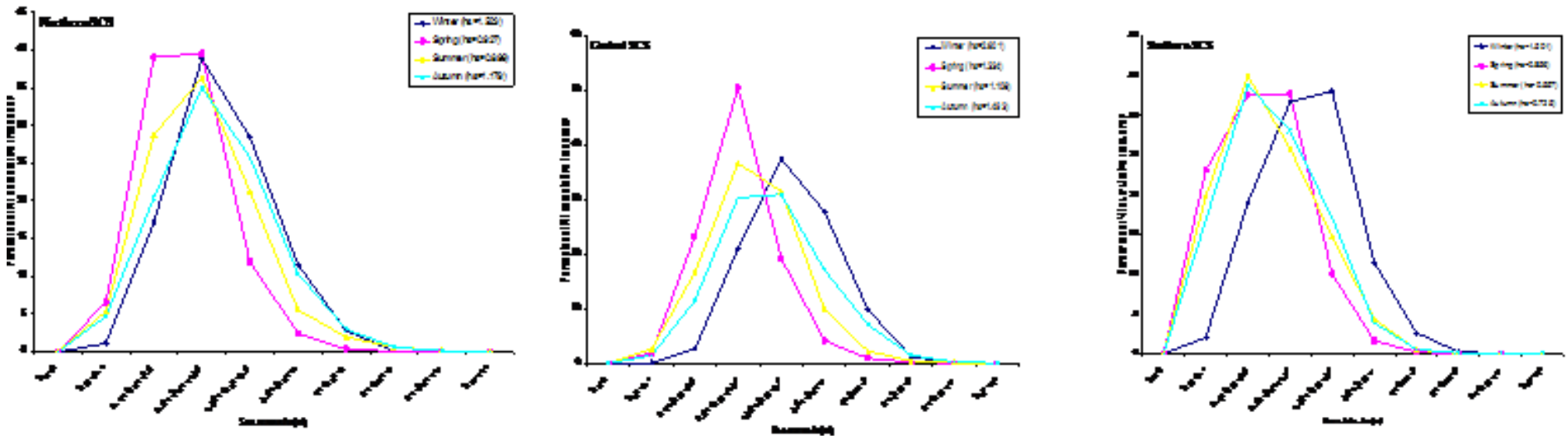


Figure 5. Seasonal average hs cumulative distribution curves for the (a) Northern, (b) Central and (c) Southern SCS. The numerical values in the legend indicate the average hs.

and autumn. In the northern SCS, the curves are nearly identical for all seasons with the exception of the curve for spring that slightly falls out of tune. This is to generally infer that localities with equal hs values have seasonal sea state curves that are nearly identical.

The hs curves can be utilized to determine the approximate sea state that is prevalent in a particular region of the SCS. The use of these seasonal hs curves to establish approximate statistical distribution of the seasonal hs for other locations within similar latitude and longitude highlights their relevance.

CONCLUSION

In this paper, a 30 year (1976-2005) SWH data obtained by simulations over some selected locations in the SCS have been utilized to

investigate the sea conditions particular to the northern, central and southern SCS. The monthly variation of the significant wave height for the selected locations has also been investigated. Results showed that the significant wave height has its minimum values in May and maximum values around November to January. Statistical analysis of the daily significant wave height and subsequent characterization of the sea states based on this were also done. Results showed that in the northern SCS, the slight sea state ($0.5 \leq h_s \leq 1.25$) has the highest frequency of occurrence. The smooth (wavelets) sea state ($0.1 \leq h_s \leq 0.5$) prevail in the southern SCS while both the moderate ($1.25 \leq h_s \leq 2.5$) and slight sea states prevail in the central SCS.

ACKNOWLEDGEMENTS

This work is financially supported by the National

Natural Science Foundation of China (51479183, 51509226), and the fundamental research funds for the central universities (201513040).

REFERENCES

Chu PC, Cheng KF (2008). South China Sea wave characteristics during Typhoon Muifa passage in winter 2004. *J. Oceanogr.*, 64(1): 1-21.
 Chu PC, Lu SH, Liu WT (1999). Uncertainty of the South China Sea prediction using NSCAT and NCEP winds during tropical storm Ernie 1996. *J. Geophys. Res.*, 104(11): 273-11 289.
 Edmons NL, Fan CW (1999). Dynamical mechanisms for the South China Sea seasonal circulation and thermohaline variabilities. *J. Phys. Oceanogr.*, 29: 2971-2989.
 Veneziano JM, Fan CW (2000). Response of the South China Sea to tropical cyclone Ernie 1996. *J. Geophys. Res.*, 105(13):991-14 009.
 Wang XL, Zwiers FW, Swail VR (2004). North Atlantic Ocean wave climate change scenarios for the twenty-first century. *J. Clim.* doi:10.1175/1520-0442.

- Rodriguez G, Guedes SC (2000). Wave period distribution in mixed sea states. Proceedings of the 19th International conference on offshore mechanics and Arctic Engineering, ASME, New York Paper OMAE 2000 /S&R-6132. conference on offshore mechanics and Arctic Engineering,
- Strekalov S, Massel S (1971). On the spectral analysis of wind waves. Arch. Hydrol. Gdansk, Poland. 18: 457-485. 1971.
- Ochi MK, Hubble EN (1976). Six-parameter wave spectra. Proc. 15th Coastal Eng. Conf. pp. 301-328. 1976.
- Guedes SC (1984). Representation of double-peaked sea wave spectra. Ocean Eng., 11: 185-207.
- Guedes SC (1992). Spectral modeling of sea states with multiple wave systems. Journal of Offshore Mechanics and Arctics Engineering, 114.
- Torsethaugen (1993). A two peak wave spectrum model. Proc. 12th Internat. Conf. Offshore Mechanics and Arctic Engineering, ASME2: pp. 175-180.
- Torsethaugen K (1996). Model for double peaked wave spectrum. Rep. No. STF 22A96204, SINTEF, Civil and Environmental Engineering, Trondheim, Norway. 1996.
- Schneggenburger C, Gunther H, Rosenthal H (2000). Spectral wave modeling with non-linear dissipation: Validation and applications in a coastal tidal environment. Coast. Eng., 41: 201-235.
- Sundar V, Ananth PN (1988). Wind climate for madras harbor, India. J. Wind Eng. Ind. Aerodynam., 31: 323-333. 1988.
- Saleh E, Beliku J, Aung T, Singh A (2010). Wave Characteristics in Sabah Waters. AmeR. J. Environ. Sci., 6(3): 219-223.
- Tolman HL (2009). User Manual and System Documentation of WAVEWATCH-III Version 3.14. NOAA/NWS/NCEP/MMAB Technical Note, Washington, 1-194. 2009.
- Fu FL, Christensen EJ, Yamaone CA, Lefebvre Y, Menard M, Dorrer P(1994). TOPEX/POSEIDON mission overview. J. Geophys. Res., 99: 24369-24381.
- Callahan PS, Morris CS, Hsiao SV (1994). Comparison of TOPEX/POSEIDON and significant wave height distributions to Geosat. J. Geophys. Res., 99: 25015-25024.
- Dobson E, Monaldo F, Goldhirsh J(1987). Validation of Geosat altimeter-derived wind speeds and significant wave heights using buoy data, J. Geophys. Res., 92: 10719-10731.